Dark Matter Search

R. Bernabei*

Dip.to di Fisica, Università di Roma "Tor Vergata"
and INFN, sez. Roma2, Rome, Italy

Lectures given at the
Summer School on Astroparticle Physics and Cosmology
Trieste, 17 June - 5 July 2002

LNS0314001

*bernabei@roma2.infn.it

Abstract

Some general arguments on the particle Dark Matter search are addressed. The WIMP direct detection technique is mainly considered and recent results obtained by exploiting the annual modulation signature are summarized.

Contents

1 Evidence and nature of Dark Matter in the Universe

The first evidence that much more than the visible matter should fill the Universe dates back to 1933 when F. Zwicky measured the dispersion velocity in the Coma galaxies [1]. This was soon after confirmed by S. Smith studying the Virgo cluster [2]. Nevertheless, only about 50 years later the fact that Dark Matter should be present in large amount in our Universe finally reached a wide consensus. It is worth to mention the contribution given in the seventies by two groups which systematically analysed the dispersion velocity in many spiral galaxies [3]: plotting the velocities in the galaxy plane as a function of distance from the galactic center, they found that the velocity curves stay flat even outside the luminous disk, pointing out the presence of a dark halo. The progresses in the astronomical observations with time passing have also offered several other experimental evidences for the Dark Universe, such as: i) the Large Magellanic Cloud spins around our Galaxy faster than expected in case only luminous matter would be present; ii) the observation of X-ray emitting gases surrounding elliptical galaxies; iii) the velocity distribution of hot intergalactic plasma in clusters. All these observations have further shown that the mass of the Universe should be much larger than the luminous one in order to explain the observed gravitational effects [4].

The existence of the Dark Universe is supported also by the standard cosmology (based on the assumption that the Universe arose from an initial singularity and went on expanding) in the inflationary scenario (proposed to avoid any fine tuning in the Big Bang initial conditions), which requires a flat Universe with density equal to the critical one: $\rho_c = \frac{3H_0^2}{8\pi G} = 1.88h^2 \cdot 10^{-29}$ g $\cdot$ cm^{-3}, where H_0 is the Hubble constant equal to $100h$ kms^{-1}Mpc^{-1} and $0.55 < h < 0.75$; the uncertainty is due to the measurements of the actual value of the expansion rate of the Universe and to the considered models [5]. Recently, the results from the balloon-borne experiments, BOOMERANG and MAXIMA, and from ground-based experiments using radio detectors and interferometry, have probed the small scale anisotropy of the cosmic microwave background by studying the power spectrum of its angular distribution. In particular, they support $\Omega = \frac{\rho}{\rho_c} = 1$ [6] and – being the average density of the Universe as measured by photometric methods: $\Omega \simeq 0.007$ (suggesting instead an open Universe which will expand forever) – they re-

quire the existence of Dark Matter in the Universe as well [1].

As regards our Galaxy, from dynamical observations one can derive that it is wrapped in a dark halo, whose density nearby the Earth has been estimated to be: $\rho_{halo} \simeq (0.3 - 0.7)$ GeV cm^{-3} [8].

The investigation on the nature of the Dark Universe has shown that large part of it should be in non-baryonic form. In fact, the mean density of baryons in term of the critical one, Ω_b, evaluated from the primordial amount of light elements (^{4}He,^{3}He,^{7}Li, ^{2}H, H) allows to derive the ratio, η, between the number of baryons and photons. Thus, knowing the photon density from the CMB measurements, in a standard model one obtains: $1.5 \times 10^{-10} < \eta < 6.3 \times 10^{-10}$, i.e. $5 \times 10^{-3} < \Omega_b h^2 < 2.4 \times 10^{-2}$ (the crucial role played by experimental results constraining the h value is evident); assuming here cautiously $h = 0.5$ (although its present estimate is larger) one gets: $\Omega_b < 0.1$ (a more plausible result would be $\Omega_b < 0.06$). At present results, for example, from experiments searching for massive compact halo objects as baryonic candidates for Dark Matter are consistent with these values; in fact, the EROS experiment quotes an exclusion plot, while the MACHO experiment gives an allowed region but for objects with masses above the ignition threshold of a star, thus for still luminous matter [9]. It is worth to remind a further argument, which also supports that the major part of the Dark Matter in the Universe should be in non-baryonic form: it is very difficult to build a model of galaxy formation without the inclusion of non-baryonic Dark Matter.

Thus, a significant role should be played by relic particles from the Big Bang. They must be stable or with a lifetime comparable with the age of the Universe to survive up to now in a significant amount; they must be neutral to be undetectable by electromagnetic interactions and their cross section with ordinary matter should be weak (in fact, if their annihilation rate would be greater than the Universe expansion rate, they should disappear). The Dark Matter candidate particles are classified in *hot* Dark matter (particles relativistic at decoupling time with masses $\lesssim$ 30 eV) and in *cold* Dark Matter (particles non relativistic at temperatures greater than 10^4 K with masses from few GeV to the TeV region or axions generated by

[1] For the sake of completeness, we mention that in last years a study has been performed on astronomical standard candles as supernova type IA, which seems to support an Universe whose expansion is accelerating. Therefore, presence of Dark energy seems to be supported [7]. If this scenario would be confirmed, the (luminous plus Dark) matter density in the Universe, Ω_m, would be 0.2 - 0.5.

symmetry breaking during primordial Universe). The light neutrinos are the natural candidates for *hot* Dark Matter; they can explain the large structure formation, but can hardly account for the galaxies formation. In particular, a pure *hot* Dark Matter scenario is ruled out by the measurements of the CMB radiation, which does not show sufficiently large inhomogeneity. Thus, *cold* Dark Matter candidates, which can be responsible for the initial gravitational collapse, should be present and in large amount, although a pure *cold* Dark Matter scenario seems to be not favoured by the observed power spectrum of density perturbation. In practice, a mixed Dark Matter scenario is generally favourably considered with – naively – 69% of *cold*, 30% of *hot* and 1% of baryonic Dark Matter. However, other possibilities can be considered such as, for example, the so-called "tilted Dark matter scenario" that introduces a significant deviation from the Zeldovich scale invariance of the power spectrum of the initial fluctuations. Anyhow, in all of the possible scenario a significant fraction is expected to be in form of *cold* Dark Matter particles.

As mentioned above, *cold* Dark Matter can be in form of axions or WIMPs (Weakly Interacting Massive Particles). The axions are light bosons, hypothesized to solve the CP problem in strong interactions; direct detection experiments are in progress since time by studying their interactions with strong electromagnetic field; no positive evidence has been found so far [10]. For completeness, we mention that some other experiments have investigated the possible axion production in the Sun [11] and some other will be realized in near future; however, these latter experiments cannot be classified as experiments for Dark matter direct detection since they are not searching for relic axions.

In the following we will address only the WIMP candidates and mainly results on their direct detection [2].

The WIMPs are particles in thermal equilibrium in the early stages of the Universe, decoupling at freeze out temperature. Considering the WIMP particles as stable and with same initial density for particles and antiparticles, their annihilation cross section, σ_{ann}, should be lower than the expansion rate of the Universe: $< \sigma_{ann} \cdot v > \simeq \frac{10^{-26}}{\Omega_{WIMP} \cdot h^2} cm^3 s^{-1}$, where v is the relative

[2]For the sake of completeness, we remind that also more exotic candidates (which generally could account for small fraction of Dark Matter in the galactic halo) have been considered and searched for such as e.g. the magnetic monopole with mass 10^{16} - 10^{17} GeV [12], the neutral Strongly Interacting Massive particles (SIMPs) [13, 14], the Q-balls [15], etc.

velocity of the particle-antiparticle pair [3]; thus, the interaction cross section results to be of the same order as the weak interaction one.

The velocity-spatial distribution of the WIMPs in our galactic halo is not well known. So far the simplest, non-consistent and approximate isothermal sphere model has been generally considered; under this assumption the WIMPs form a dissipationless gas trapped in the gravitational field of our Galaxy in an equilibrium steady state and have a quasi-maxwellian velocity distribution with a cut-off at the escape velocity from the galactic gravitational field. It is worth to remark that more realistic halo models have been proposed by various authors such as Evans' power-law halos, Michie models with an asymmetric velocity distribution, Maxwellian halos with bulk rotation, etc. [16]. In particular, a devoted discussion on a wide (but still not complete) number of consistent halo models and their implications on available data has been carried out recently in ref. [17].

The more widely considered candidate for WIMPs is at present the lightest supersymmetric particle named neutralino, χ. In the MSSM, where R-parity is conserved, heavier SUSY particles decay into lighter ones; thus, χ must be stable and cannot interact neither by electromagnetic nor by strong interactions, otherwise it would condensate and would be detected in the galactic halo with the ordinary matter. In the MSSM, the χ is defined as the lowest-mass linear combination of photino ($\tilde{\gamma}$), zino ($\tilde{Z}$) and higgsinos ($\tilde{h}_1, \tilde{h}_2$): $\chi = a_1\tilde{\gamma} + a_2\tilde{Z} + a_3\tilde{h}_1 + a_4\tilde{h}_2$ where $\tilde{\gamma}$ and $\tilde{Z}$ are linear combination of U(1) and SU(2) neutral gauginos, $\tilde{B}$ and $\tilde{W}_3$: $\tilde{\gamma} = cos\theta_W \cdot \tilde{B} + sin\theta_W \cdot \tilde{W}_3$ and $\tilde{Z} = -sin\theta_W \cdot \tilde{B} + cos\theta_W \cdot \tilde{W}_3$ with θ_W Weinberg angle. The χ is a Majorana particle. The χ mass and the a_i coefficients depend on the Higgs mass mixing parameter, μ, on the $\tilde{B}$ and $\tilde{W}_3$ masses and on $tg\beta$, the ratio between the v.e.v's which give masses to up and down quarks. Thus, often the experimental results are presented in terms of μ, $tg\beta$ and wino mass, M_2. The χ cross section on ordinary matter is described by three Feynman diagrams: i) exchange between χ and quarks of the ordinary matter through Higgs particles (spin-independent – SI – interaction); ii) exchange between χ and quarks of the ordinary matter through Z^0 (spin-dependent – SD – interaction); iii) exchange between χ and quarks of the ordinary matter through squark (mixed – SI/SD – interaction). It is worth to note that the evaluation of the expected rates for χ depends on several parameters and procedures, which are affected by significant uncertainties, such as

[3] In case the particles and antiparticles would not have the same initial density, this relation would represent a lower limit.

e.g. the considered neutralino composition, the present uncertainties on the measured top quark mass and on certain sectors of the fundamental nuclear cross sections, some lack of information about physical properties related to Higgs bosons and SUSY particles, the possible use of constraints from GUT schemes and/or from $b \to s+\gamma$ branching ratio, the used rescaling procedure, etc.; in conclusion, considering also the large number of involved parameters, the supersymmetric theories have no practical predictive capability.

Other candidates can also be considered as WIMPs; as an example we remind an heavy neutrino of a 4-th family [18] and the sneutrino in the scenario proposed by ref. [19].

As regards their detection, the WIMPs can be investigated for either by direct or by indirect methods. In the first case, their elastic interaction on target nuclei can be detected deep underground by means of the signal induced by the recoiling nucleus or, in case of inelastic scattering, also by the successive de-excitation gamma's. In the other case, the flux of secondary particles - mainly neutrinos, positrons, gamma's - produced by possible WIMP annihilation in the Sun, in the Earth or in the halo can be detected. Indirect searches can be performed by satellite, balloon, terrestrial, underwater or underground experiments.

In the following we will mainly focus our attention on the direct detection technique in underground laboratory, where the low environmental background can allow to reach the highest sensitivity. However, we will preliminary briefly recall few main points on the indirect detection approach.

2 Generalities on indirect searches for WIMPs

It has been suggested that Dark Matter particles could loose their velocity down to a value lower than the escape velocity of a celestial body (Earth, Sun) scattering off a nucleus and, therefore, remaining trapped in its gravitational field. Subsequently, via their annihilation in the celestial bodies (Earth, Sun) or in the Galactic halo [4] they could give rise to high energy neutrinos, positrons, antiprotons and gamma's. In principle, the Sun could capture WIMPs more effectively than the Earth because of the higher escape velocity, but the smaller distance detector – center of the Earth and the "resonant" scattering on the heavy nuclei in the Earth (mostly on iron) could compensate this effect.

[4] Generally it is assumed that the capture rate would be equal to the rate of the WIMP annihilation.

The best signature is expected from ν_μ interacting in the rock below a detector producing "upgoing" muons in the detector itself. The expected μ flux depends on the WIMP annihilation rate in the Sun or in the Earth and on the ν energy spectrum produced in the annihilations. Thus, several source of uncertainties are present in similar estimates (and, therefore, in the obtained results) such as for example the assumption that a "steady state" has been reached in the considered celestial body and the significant uncertainty which arises from the estimate and subtraction of the existing competing process offered by the atmospheric neutrinos.

Anyhow, when a model is assumed as well as the related parameters' values, it is possible to estimate the differential flux expected for the secondary neutrinos. According to ref. [20] (where the neutralino in the MSSM model has been considered), this flux can be written as

$$\frac{dN_\nu}{dE_\nu} = \frac{\Gamma_A}{4\pi d^2} \sum_{F,f} B_{\chi f}^{(F)} \frac{dN_{f\nu}}{dE_\nu} \tag{1}$$

where Γ_A is the annihilation rate, d is the distance between the detector and the source (e.g. the Earth center or the Sun center), F is the final state of the annihilation process, $B_{\chi f}^{(F)}$ are the branching ratios of the heavy quarks decays; the $dN_{f\nu}/dE_\nu$ term represents the differential distribution of neutrinos produced by τ and by the quarks and gluons adronization and of the subsequent semileptonic decays of the produced hadrons.

Considering, in particular, the ν_μ and $\overline{\nu}_\mu$, an estimate of the produced neutrino flux can be obtained by measuring the up-going muons given by the ν_μ and $\overline{\nu}_\mu$ interactions with the rock surrounding the detector. Their energy distribution can be written as:

$$\frac{dN_\mu}{dE_\mu} = N_A \int_{E_\mu^{th}}^{\infty} dE_\nu \int_0^{\infty} dX \int_{E_\mu}^{E_\nu} dE'_\nu P_{surv}(E_\mu, E'_\mu; X) \frac{d\sigma(E_\mu, E'_\mu)}{dE'_\mu} \frac{dN_\nu}{dE_\nu} \tag{2}$$

where X is the muon range in the rock, $d\sigma(E_\mu, E'_\mu)/dE'_\mu$ is the charge current cross section for muon production of energy E'_μ from a neutrino of energy E_ν and $P_{surv}(E_\mu, E'_\mu; X)$ is the survival probability of a muon with E'_μ initial energy and E_μ final energy after crossing a thickness X of rock; E_μ^{th} is, finally, the energy threshold of the detector. The function $P_{surv}(E_\mu, E'_\mu; X)$ obviously account for the muon energy loss in the rock.

The up-going muons produced by atmospheric neutrinos are side reactions for the process searched for, however – in principle – they are expected

to have a flat angular distribution while those induced by WIMPs have a preferred impinging direction (e.g. the Sun–laboratory direction or Earth center–laboratory direction).

Model dependent analyses with a similar approach have been carried out by large experiments deep underground such as e.g. MACRO and Superkamiokande. It is worth to remark that no quantitative comparison can be directly performed between the results obtained in direct and indirect searches because it strongly depends on the assumptions and on the considered model frameworks. In particular, a comparison would always require the calculation and the consideration of all the possible WIMP configurations in the given particle model (e.g. for χ: in the allowed parameters space), since it does not exist a biunivocal correspondence between the observables in the two kinds of experiments: WIMP-nucleus elastic scattering cross section (direct detection case) and flux of muons from neutrinos (indirect detection case). In fact, the counting rate in direct search is proportional to the spin-dependent (SD) and to the spin-independent (SI) cross sections, while the muon flux is connected not only to them, but also to the WIMP annihilation cross section. In principle, the three cross sections can be correlated, but only when a specific model is adopted and by non directly proportional relations. As an example, we report in Fig. 1 the scatter plot for the up-going muon flux from the center of the Earth for a standard Maxwellian distribution versus χ mass in MSSM [21]. There the configurations have been selected by the DAMA annual modulation region for the particular purely SI model framework given in [22]; as it is evident, the up-going muon flux spans several orders of magnitude although the DAMA region in this model framework spans almost one. The solid line in this figure is the model dependent upper bound derived from MACRO experiment [23]; the one from Superkamiokande is only marginally more stringent, thus it is still compatible with the DAMA result (even when the uncertainties on several assumptions and parameters are not yet included).

For the sake of completeness, we recall that the search for up-going muons from similar processes has been planned since long time to be realized underwater or under-ice. Several R&D's (e.g. DUMAND, NESTOR, ANTARES, NEMO) have been and are carried out so far as well as the AMANDA and lake Baikal experiments [24]. However, the objective difficulties in operating for long time with a very-large-surface set-up in full controlled situation do not allow, at present, a realistic prevision for possible future operation of a km^2 surface detector, which is the present goal of various R&D's.

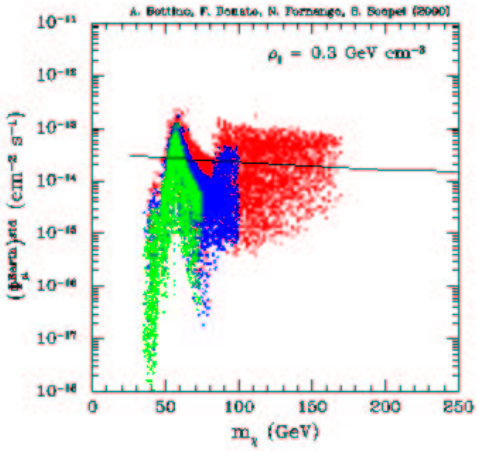

Figure 1: Scatter plot for the up-going muon flux from the center of the Earth for a standard Maxwellian distribution vs neutralino mass. The configurations (MSSM) have been selected by the DAMA annual modulation region for the model framework considered in ref. [22]. For details see [21]. The solid line is the model dependent upper bound derived from MACRO experiment; the one from Superkamiokande is only marginally more stringent.

As we mentioned at the beginning, the annihilation of Dark Matter particles in the halo could also produce antimatter particles and gamma's. The antimatter searches have to be carried out outside the atmosphere, i.e. on balloons or satellites. In particular, the WIMP annihilation would result in an excess of antiprotons or of positrons up to the WIMP mass with respect to the background arising from other possible sources. Again the estimate and subtraction of such a background together with the influence of the Earth and of the galactic magnetic field on these particles plays a crucial role on the possibility of a reliable extraction of a signal. However, at present some interesting result has been reported in the analysis of the HEAT balloon-borne experiment. In fact, an excess of positrons has been found, which – if interpreted in term of WIMP annihilation [25] – gives a result not in conflict with the effect observed by DAMA (see later). Further results can be expected in future by experiments operating in space [26].

As regards the possibility to detect γ's from WIMP annihilation in the galactic halo, experiments in space are planned. However, at present it is difficult to estimate their possibilities considering e.g. the huge background level, the uncertainties in its reliable estimate and subtraction as well as the

smallness of the expected signal (considering the already achieved sensitivity by direct searches and, even more, if a subdominant component is present) when properly calculated with rescaling procedure. However, we mention the analysis of ref. [27] which suggest the presence of a γ excess from the center of the Galaxy in the EGRET data [28]. This has been interpret as a possible contribution from a neutralino with mass of about 102 GeV [27]. Also this analysis which has been performed after the DAMA annual modulation result give a mass compatible with the effect observed by DAMA. Other activities are in preparation [29].

3 Generalities on WIMPs direct detection

A direct search for Dark Matter particles requires: i) a suitable deep underground site to reduce at most the background contribution from cosmic rays; ii) low background hard shields against electromagnetic and neutron background; iii) the selection of low background materials and the identification of radio-purification techniques to build low background set-ups; iv) effective Radon removal systems; v) a good model independent signature.

As an example of the suitable performances of a deep underground laboratory we quoted here those measured at the Gran Sasso National Laboratory of I.N.F.N.: i) muon flux: 0.6 muons m^{-2} h^{-1}; ii) thermal neutron flux: 1.08 $\cdot 10^{-6}$ neutrons cm^{-2} s^{-1}; iii) epithermal neutron flux: 1.98 $\cdot 10^{-6}$ neutrons cm^{-2} s^{-1}; iv) fast ($E_n > 2.5 MeV$) neutron flux: 0.09 $\cdot 10^{-6}$ neutrons cm^{-2} s^{-1}; v) Radon in the hall: $\simeq$ 10-30 Bq m^{-3}.

The low background technique requires very long and accurate work for the selection of low radioactive materials by sample measurements with HP-Ge detectors (placed deep underground in suitable hard shields) and/or by mass spectrometer analyses. Thus, these measurements are often difficult experiments themselves, depending on the required radiopurity. Moreover, uncertainties due to the sampling procedure and to the subsequent handling of the materials to build the apparata also require further time and efforts. As an example of an investigation of materials and detector radiopurity, one can consider ref. [30] where the residual radioactivity measured in materials and detectors developed for the $\simeq$ 100 kg highly radiopure NaI(Tl) DAMA set-up is reported; some discussion on how to further improve the radiopurity of NaI(Tl) detectors can be found e.g. in ref. [31]. Furthermore, an interesting paper on the low background techniques is e.g. [32]. It is worth to note that generally main efforts regard the reduction of standard contam-

inants: ^{238}U and ^{232}Th (because of their rich chains) and ^{40}K (because of its large presence in nature). When suitable radiopurity is reached for these components, one should investigate the possible presence of non-standard contaminants by devoted measurements. As reported e.g. in ref. [33], several orders of magnitude of rate reduction can be obtained with time and efforts in improving the experimental conditions.

More recently, strategies to reject electromagnetic background from the data have been pursued to try to overcome the long and difficult work of developing very low background set-ups. This can be realized in several scintillators by pulse shape discrimination (since electrons show a different decay time than nuclear recoils, such as e.g. in NaI(Tl) and LXe) or comparing two different signals collected for the same events (if they have different expected recoil/electron response ratio, such as heat/ionization in Ge or Si and heat/light in CaF_2(Eu), $CaWO_4$). The first case offers a relatively safer approach since basic quantities (such as e.g. the sensitive volume) are well defined, while the second is more uncertain requiring e.g. the precise knowledge of the effective sensitive volume for both signals. A further discrimination strategy, which uses a two-phases gas/liquid Xenon detector with an applied electric field has been also suggested; there the light amplitudes of the primary and of the secondary scintillation pulses are compared. However, in this case the discrimination critically depends e.g. on the definition of the real sensitive volume, on the dependence of the discrimination power with ionization position, gas purity etc. In every case, whatever strategy is followed, always only a statistical discrimination is possible (on the contrary of what is often claimed) because e.g. of tail effects from the two populations, from the noise, etc. Furthermore, the existence of concurrent processes (due e.g. to end-range alphas, neutrons or in some case also by so–called surface electrons) excludes that an unambiguous result can be obtained for WIMP presence with this approach. Finally, a similar strategy cannot be pursued when a signature based on the correlation of the measured experimental rate with the Earth galactic motion is pursued (see later); in fact, the effect searched for (which is typically at level of few %) would be largely affected by the uncertainties associated to the – always statistical – discrimination procedure. As an example of reduction obtainable by pulse shape analysis, in Fig. 2 the results reported in ref. [34] considering the data collected by the $\simeq$ 6.5 kg DAMA Liquid Xenon experiment are shown. The proper knowledge of other quantities is also necessary for a WIMP direct search such as e.g. the recoil/electron response ratio for the given nucleus in the given detector,

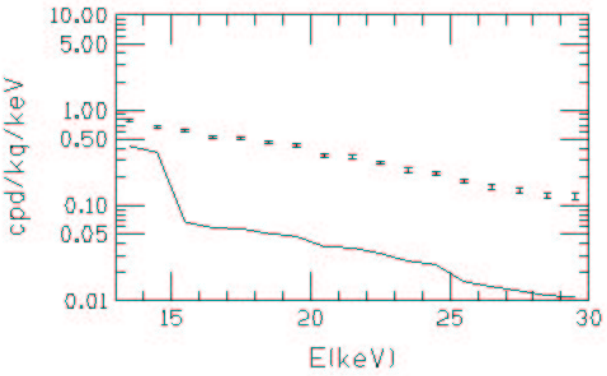

Figure 2: Result obtained by applying the pulse shape discrimination procedure to the data collected by a Liquid Xenon pure scintillator [34]: the points represent measured rates, while the continuous line represents the upper limits at 90% C.L. obtained for the recoil fractions [34].

the possibility of a reliable identification of the energy threshold and of the residual noise above it (as it can be effectively done in NaI(Tl) detectors with adequate number of photoelectrons/keV; see e.g. [30]). Generally, the recoil/electron response ratio is measured with neutron source or at neutron generator (see e.g. [35]). In the latter case a set-up similar to Fig. 3 is used with a quasi-monochromatic neutron beam and the scattered neutrons are tagged. It is worth to note that significant differences are often present in literature for the measured value of this ratio for the same nucleus in similar detectors. This is generally due to different peculiarities of the detectors themselves; for example, in doped scintillator it can depend on the dopant concentration, in liquid Xenon on the residual trace contaminants and in Ge or Si on impurities, etc. Let us, finally, comment that while this configuration works out well for the measurements of recoil/electron responses ratio, it is unsuitable to determine the absolute detection efficiency for recoils because of the uncertain knowledge of the elastic cross sections, of the background due to inelastic scatterings, of the electromagnetic and hadronic background from neutron interaction in the environment, of the cuts for noise rejection in a very high rate environment, of the duty cycle (which is very small), etc.

We remind that a WIMP signal can be searched for by investigating the WIMP-nucleus inelastic scattering, producing low-lying excited nuclear states. In this case, as a result of the emission of successive de-excitation gamma rays from the excited nuclear states, the presence of characteristic

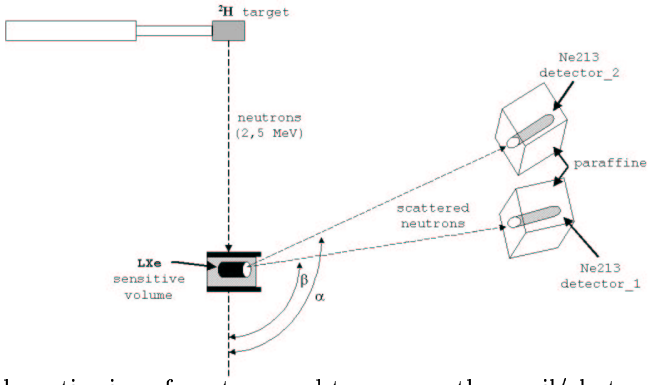

Figure 3: Schematic view of a set-up used to measure the recoil/electron response ratio in a given detector [35].

peaks in the measured energy spectrum can be searched for. This approach can offer distinctive evidence for WIMP, but very large exposures are necessary to reach a significantly high sensitivity. For this reason only few experimental works have been carried out so far [36, 37, 38].

In the following we will devote our attention to the case for WIMP direct detection by elastic scattering deep underground, since this technique has offered so far the highest sensitivity. Thus, the studied process is the WIMP-nucleus elastic scattering and the quantity measured in underground set-ups is the recoil energy.

4 WIMP direct detection by elastic scattering

The differential energy distribution of the recoil nuclei can be calculated [21, 39] by means of the differential cross section of the WIMP-nucleus elastic processes

$$\frac{d\sigma}{dE_R}(v, E_R) = \left(\frac{d\sigma}{dE_R}\right)_{SI} + \left(\frac{d\sigma}{dE_R}\right)_{SD} =$$

$$= \frac{2G_F^2 m_N}{\pi v^2}\{\left[Zg_p + (A-Z)g_n\right]^2 F_{SI}^2(E_R) + 8\Lambda^2 J(J+1)F_{SD}^2(E_R)\} \qquad (3)$$

where: G_F is the Fermi coupling constant; m_N is the nucleus mass; v is the WIMP velocity in the laboratory frame; $E_R = m_{WN}^2 v^2(1 - cos\theta^*)/m_N$ (with m_{WN} WIMP-nucleus reduced mass and θ^* scattering angle in the c.m. frame) is the recoil energy; Z is the nuclear charge and A is the atomic number; $g_{p,n}$ are the effective WIMP-nucleon couplings for SI interactions;

$\Lambda^2 J(J+1)$ is a spin factor. Moreover, $F_{SI}^2(E_R)$ is the considered SI form factor (see e.g. ref. [40]). As regards the SD form factor, $F_{SD}^2(E_R)$, an universal formulation is not possible; in fact, in this case the internal degrees of the WIMP particle model (e.g. supersymmetry in case of neutralino) cannot be completely separated from the nuclear ones and different nuclear potential can be considered [41]. It is worth to note that this adds significant uncertainty in the results.

It can be demonstrated that $\Lambda = \frac{a_p<S_p>+a_n<S_n>}{J}$ with J nuclear spin, $a_{p,n}$ effective WIMP-nucleon couplings for SD interaction and $< S_{p,n} >$ mean value of the nucleon spin in the nucleus. Therefore, the differential cross section and, consequently, the expected energy distribution depends on the WIMP mass and on four unknown parameters of the theory: $g_{p,n}$ and $a_{p,n}$.

It is convenient to introduce a generalized SI WIMP-nucleon cross section: $\sigma_{SI} = \frac{4}{\pi} G_F^2 m_{Wp}^2 g^2$, where $g = \frac{Zg_p+(A-Z)g_n}{A} = \left(\frac{g_p+g_n}{2}\right)\left[1 - \frac{g_p-g_n}{g_p+g_n}\left(1 - \frac{2Z}{A}\right)\right]$. Since $\frac{Z}{A}$ is nearly constant for the nuclei typically used in WIMP direct detection, the coupling term g can be assumed – in a first approximation – as independent on the used target nucleus.

We consider the useful notations [42]: $\bar{a} = \sqrt{a_p^2 + a_n^2}$, $tg\theta = \frac{a_n}{a_p}$, $\sigma_{SD} = \frac{32}{\pi}\frac{3}{4} G_F^2 m_{Wp}^2 \bar{a}^2$, where σ_{SD} is a suitable SD WIMP-nucleon cross section.

In conclusion, equation (1) can be re-written in terms of σ_{SI}, σ_{SD} and θ as:

$$\frac{d\sigma}{dE_R}(v, E_R) = \frac{m_N}{2m_{Wp}^2 v^2} \cdot \Sigma(E_R) \tag{4}$$

with $\Sigma(E_R) = \{A^2 \sigma_{SI} F_{SI}^2(E_R) + \frac{4}{3}\frac{(J+1)}{J}\sigma_{SD}[< S_p > \cos\theta + < S_n > \sin\theta]^2 F_{SD}^2(E_R)\}$. The mixing angle θ is defined in the $[0, \pi)$ interval; in particular, θ values in the second sector account for a_p and a_n with different signs. As it can be noted from its definition [21], $F_{SD}^2(E_R)$ depends on a_p and a_n only through their ratio and, consequently, depends on θ, but it does not depend on $\bar{a}$.

Finally, setting the local WIMP density, ρ_W, and the WIMP mass, m_W, one can write the energy distribution of the recoil rate (R) in the form

$$\frac{dR}{dE_R} = N_T \frac{\rho_W}{m_W} \int_{v_{min}(E_R)}^{v_{max}} \frac{d\sigma}{dE_R}(v, E_R) v f(v) dv = N_T \frac{\rho_W \cdot m_N}{2 m_W \cdot m_{Wp}^2} \Sigma(E_R) I(E_R), \tag{5}$$

where: N_T is the number of target nuclei and $I(E_R) = \int_{v_{min}(E_R)}^{v_{max}} dv \frac{f(v)}{v}$ with $f(v)$ WIMP velocity distribution in the Earth frame [21]; $v_{min} = \sqrt{\frac{m_N \cdot E_R}{2m_{WN}^2}}$ is the minimal WIMP velocity providing E_R recoil energy; v_{max} is the maximal WIMP velocity in the halo evaluated in the Earth frame. The extension of formula (5) e.g. to multiple nuclei detectors can be easily derived.

4.1 The "traditional" approach

Since often the used statistics in direct experiments is very poor, the simple comparison of the measured energy distribution with an expectation from theory is carried out. This "traditional" approach – the only one which can be pursued by small scale or poor duty cycle experiments – allows only to calculate model dependent limits on WIMP-nucleus cross section at given C.L.

Although for long time the limits achieved by this approach have been presented as robust reference points, it can be easily understood that similar results are quite uncertain not only – as always – because of possible underestimated or unknown systematics in the data, but also because the result refers only to a specific model framework. This is identified not only by the general astrophysical, nuclear and particle physics assumptions but also by the set of values used in the calculations for the needed theoretical and experimental parameters (such as WIMP local velocity, v_0, form factors parameters, quenching factor, etc.), which are instead also affected by uncertainties. As an example, Fig. 4 shows how an exclusion plot is modified by changing (within the intervals allowed by the present determinations) the values of the astrophysical velocities [43]. Analogous effect will be obtained when varying – within allowed values – every other of the several needed parameters as well as, obviously, when varying every one of the general assumptions. In Fig. 5a) as an example SI form factors used so far by various authors for the Iodine case are depicted, while in Fig. 5b) the effect of a relatively small variation (20%) of the nuclear radius, r, and the nuclear surface thickness parameter, s, in the SI form factor, calculated according to ref. [40], is shown; as it can be seen, even a relative small variation of these parameters can produce sizeable change in the behaviour of the form factor and, therefore, in the expected SI signal rate and in the final result.

As mentioned above, the situation is even more uncertain when considering the SD case since the nuclear and particle physics parameters cannot be decoupled. As an example, in Fig. 6a) some SD form factors considered

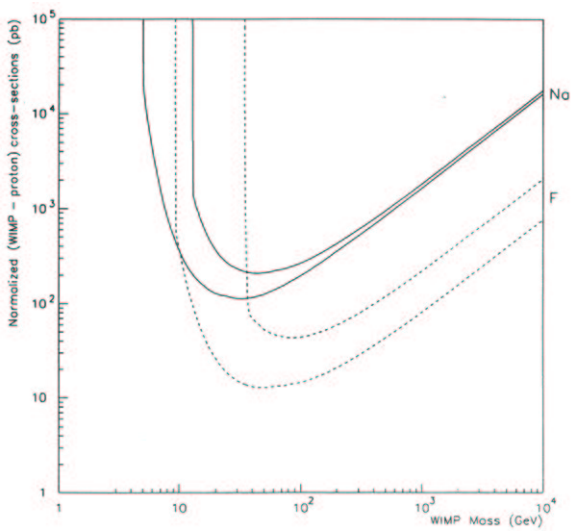

Figure 4: Example of the effects due to the uncertainties of the halo velocity and of the escape velocity in a result for spin-dependent coupled WIMP [43]. Here the cases of Sodium and Fluorine are considered as examples. The top curve for each nucleus has been calculated for $v_0 = 180$ km/s and $v_{esc} = 500$ km/s, while the lower curve has been calculated for $v_0 = 250$ km/s and $v_{esc} = 1000$ km/s for a given model framework. Similar effects will be found for every kind of experimental result obtained in this field.

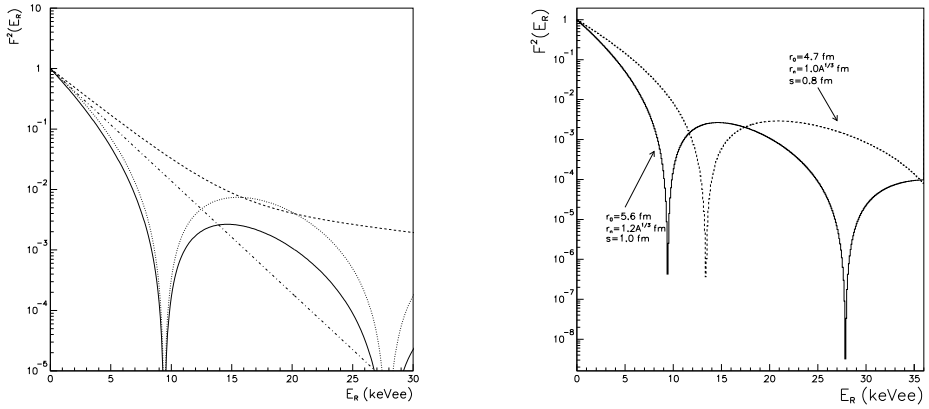

Figure 5: On the left: some SI form factors for Iodine considered so far in literature. On the right: example of variation of the SI form factor, calculated according to ref. [40], when some uncertainties on its parameters are considered; as it can be seen, even a relative small variation of these parameters can produce sizeable change in the behaviour of the form factor and, therefore, in the expected SI signal rate. Here keVee means keV electron equivalent (the used quenching factor value is that measured for the DAMA detectors).

so far for the Iodine case are depicted, while in Fig. 6b) the effect of the different choice of the nucleon-nucleon potential in the SD form factor calculated according to ref. [41] is shown. Similar uncertainties are present for every kind of nucleus. Finally, let us note that typically only purely SI or

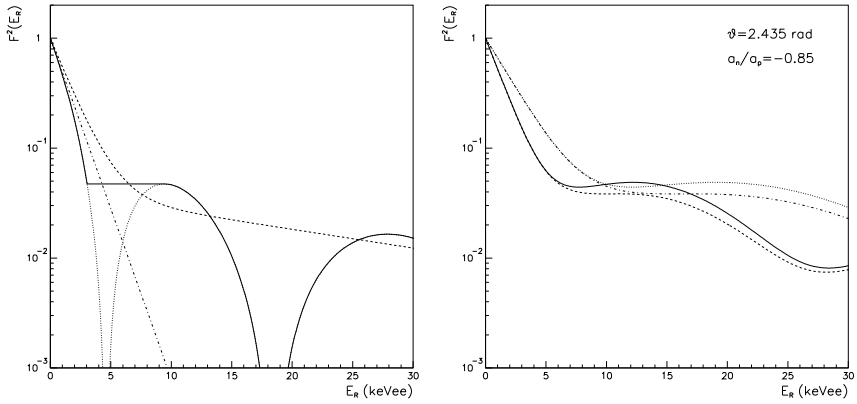

Figure 6: On the left: some SD form factors for Iodine considered so far. On the right: example of variation of the SD form factor, calculated according to ref. [41] for two different choice of the nucleon-nucleon potential, when a possible small variation (20%) of its parameter is considered. As it can be seen, even a relative small variation either of this parameter or o=in the nuclear potential can produce sizeable change in the behaviour of the form factor and, therefore, in the expected SD signal rate.

purely SD Z^0 coupling WIMP interactions are considered with respect to all the wide available possibilities.

The uncertainty largely increases when results obtained by using two different target nuclei are considered, since not only for each of them all the previous uncertainties would hold, but in addition the scaling to a common reference quantity would be necessary. In fact, WIMP-nucleus elastic cross sections on different nuclei cannot be directly compared [5]. Generally, the WIMP-nucleon cross sections σ_{SI} and σ_{SD} are considered and additional uncertainties are introduced by applying scaling laws.

In conclusion, this model dependent approach has no discovery potentiality and can give only "negative" results. Therefore, experiments offering model independent signature for WIMPs presence in the galactic halo are mandatory.

[5] We take this occasion to note that e.g. exclusion plot given in term of cross section on nucleus are not model independent as quoted sometimes, since they depend – for example – on the considered halo model.

4.2 Signatures for WIMPs

To obtain a reliable signature for WIMPs is necessary to follow a suitable model independent approach. In principle, three main possibilities exist; they are based on the correlation between the distribution of the events detected in a suitable underground set-up with the galactic motion of the Earth.

The first one correlates the recoil direction with that of the Earth velocity, but it is practically discarded mainly by the technical difficulties in detecting the short recoil track. Few R&D attempts have been carried out so far such as e.g. [44], while a suggestion, based on the use of anisotropic scintillators, was originally proposed in [45] and recently revisited [46].

The second one correlates the time occurrence of each event with the diurnal rotation of the Earth. In fact, a diurnal variation of the low energy rate in WIMP direct searches can be expected during the sidereal day since the Earth shields a given detector with a variable thickness, eclipsing the WIMP "wind" [47]. However, this effect can be appreciable only for relatively high cross section candidates and, therefore, it can only test a limited range of Cold Dark Matter halo density. For a recent experimental result see e.g. [48].

The third possibility, feasible and able to test a large range of cross sections and of WIMP halo densities, is the so-called annual modulation signature [49]. This is the main signature exploited by $\simeq$ 100 kg highly radiopure NaI(Tl) DAMA set-up [22, 42, 50, 51, 52, 53, 54]. The annual modulation of the signal rate is induced by the Earth revolution around the Sun; as a consequence, the Earth will be crossed by a larger WIMP flux in June (when its rotational velocity is summed to the one of the solar system with respect to the Galaxy) and by a smaller one in December (when the two velocities are subtracted). The fractional difference between the maximum and the minimum of the rate is of order of $\simeq 7\%$. Therefore, to point out the modulated component of the signal, large mass apparata with suitable performances and control of operating conditions – such as the $\simeq$ 100 kg highly radiopure NaI(Tl) DAMA set-up – are necessary. The annual modulation signature is very distinctive since a WIMP-induced seasonal effect must simultaneously satisfy all the following requirements: the rate must contain a component modulated according to a cosine function (1) with one year period (2) and a phase that peaks around $\simeq 2^{nd}$ June (3); this modulation must only be found in a well-defined low energy range, where WIMP induced recoils can

be present (4); it must apply to those events in which just one detector of many actually "fires", since the WIMP multi-scattering probability is negligible (5); the modulation amplitude in the region of maximal sensitivity must be $\lesssim 7\%$ (6). Only systematic effects able to fulfil these 6 requirements could fake this signature; no one has been found nor suggested by anyone.

For the sake of completeness, we comment that every kind of background rejection technique (such as PSD in scintillators, heat/ionizing and heat/light signals in bolometers) – even under the unrealistic assumption of an ideal electromagnetic background rejection – cannot allow to unambiguously identify a WIMP presence. In fact, e.g., recoils can be induced by other processes in competition with the WIMP-nucleus scattering. Moreover, tails of other kinds of populations (such as e.g. the so-called surface electrons in bolometers and the noise), the internal end-range alphas and fission fragments also generate signals indistinguishable from WIMP induced recoils. Such a contribution cannot be estimated and subtracted in any reliable manner at the needed level of precision. Thus, every result based on background rejection techniques will always be a conjecture on the real nature of the observed events. Moreover, as it can be easily understood, the possibility of a reliable investigation of model independent signatures (such as the annual modulation one) on discriminated events (whatever technique will be used) is ruled out the uncertainties existing in the rejection itself.

Most of the detection techniques, mainly in the light of a possible effective search for a WIMP signature, have been briefly commented in ref. [55]; they regards: 1) the solid scintillators; 2) the gaseous/liquid/solid noble gas detectors; 3) the ionizing Ge detectors; 4) the bolometer with electromagnetic background rejection; 5) the bolometer with heat read-out.

The following part will be devoted to summarize the DAMA result on the investigation of the WIMP annual modulation signature.

5 The DAMA result on the WIMP annual modulation

The DAMA experiment is mainly devoted to the search for rare processes (such as WIMPs direct detection, $\beta\beta$ decay processes, charge-non-conserving processes, Pauli exclusion principle violating processes, nucleon instability, solar axions and exotics [56, 57, 48, 39, 50, 30, 51, 52, 22, 53, 42, 54, 17]) by developing and using low radioactive scintillators. The main experimental

set-ups are: the $\simeq$ 100 kg NaI(Tl) set-up [30] (which has completed its data taking in July 2002), the $\simeq$ 6.5 kg liquid Xenon (LXe) set-up [57], the so-called "R&D" apparatus and the new LIBRA (Large sodium Iodine Bulk for RAre processes; $\simeq$ 250 kg of ultra-radiopure NaI(Tl)) set-up whose installation has been started in fall 2002. Moreover, an underground low-background germanium detector allows to select materials for radiopurity.

In this paper only the results obtained in the search for WIMPs by exploiting the annual modulation signature with the $\simeq$ 100 kg NaI(Tl) set-up will be discussed.

The recoil/electron light ratio for ^{23}Na and ^{127}I and the pulse shape discrimination capability have been measured by neutron source and upper limits on recoils have been measured in this set-up by exploiting the pulse shape discrimination technique [39]. Moreover, studies on possible diurnal variation of the low energy rate in the data of the $\simeq$ 100 kg NaI(Tl) set-up have also been carried out; the obtained result supports that the effect pointed out by the studies on the WIMP annual modulation signature (see later) would account for a halo fraction $\gtrsim 10^{-3}$ [48].

The main goal of the $\simeq$ 100 kg NaI(Tl) set-up is to investigate the WIMP annual modulation signature. This set-up [30] can effectively exploit such a signature because of its well known technology, of its high intrinsic radiopurity, of its mass, of its suitable control of all the operational parameters and of the deep underground experimental site.

5.1 Model independent evidence

Our solar system, which is moving with respect to the galactic system, is continuously hit by a WIMP "wind", being the WIMPs embedded in the galactic halo. Thus, they can be mainly searched for by WIMP elastic scattering on the target nuclei of a suitable detector. Moreover, since the Earth rotates around the Sun, which is moving with respect to the galactic system, it would be crossed by a larger WIMP flux in June (when its rotational velocity is summed to the one of the solar system with respect to the Galaxy) and by a smaller one in December (when the two velocities are subtracted).

This will give rise to an annual modulation of the WIMP-nucleus elastic scattering rate measured by a suitable (see above) set-up located deep underground [49], (offering in this way the possibility to point out a model independent evidence for the presence of a WIMP component in the galactic halo). This annual modulation signature (originally suggested in ref. [49])

is very distinctive; in fact, a WIMP-induced seasonal effect must simultaneously satisfy all the following requirements: the rate must contain a component modulated according to a cosine function (1) with one year period (2) and a phase that peaks around $\simeq 2^{nd}$ June (3); this modulation must be found in a well-defined low energy range, where WIMP induced recoils can be present (4); it must apply to those events in which just one detector of many actually "fires", since the WIMP multi-scattering probability is negligible (5); the modulation amplitude in the region of maximal sensitivity must be $\lesssim$7% (6). Only systematic effects able to fulfil these 6 requirements could fake this signature; no one able to do that has been found or suggested by anyone [53].

DAMA/NaI has already released so far the results obtained by investigating this annual modulation signature in the data collected during four independent experiments of one year cycle each one (of 57986 $kg \cdot day$ total statistics) [50, 51, 52, 22, 53, 42, 54, 17]; there all the peculiarities required by the signature are satisfied.

In particular, a model independent analysis of the data offers an immediate evidence of the presence of an annual modulation of the rate of the single hit events in the lowest energy interval (2 – 6 keV) as shown in Fig. 7. As it can be seen, the data of the four years give consistent results with

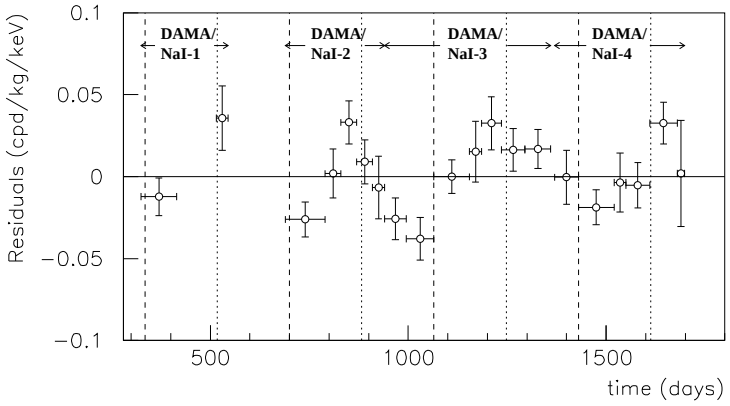

Figure 7: Model independent residual rate for single hit events, in the 2–6 keV cumulative energy interval, as a function of the time elapsed since January 1-st of the first year of data taking. The expected behaviour of a WIMP signal is a cosine function with minimum roughly at the dashed vertical lines and with maximum roughly at the dotted ones.

proper period and phase and largely disfavour the hypothesis of unmodulated behaviour [22]. No modulation is found in higher energy regions.

The results of the investigations of all the possible known systematics or side reactions have been extensively and quantitatively discussed in ref. [53]. No known systematic effect or side reaction able to mimic a WIMP induced effect has been found as quantitatively discussed in detail in ref. [53].

In conclusion, the result of the model independent approach suggests a WIMP contribution to the measured rate, independently on the nature and coupling with ordinary matter of the possible WIMP particle.

5.2 Model dependent analyses of the annual modulation data

To investigate the nature and coupling with ordinary matter of the WIMP candidate, a suitable energy and time correlation analysis is necessary as well as the assumption of one among the many possible model frameworks [6].

For simplicity, initially we have considered the particular case of purely spin-independent (SI) coupled WIMP. In fact, often the spin-independent interaction with ordinary matter is assumed to be dominant since e.g. most of the used target-nuclei are practically not sensitive to SD interactions as on the contrary ^{23}Na and ^{127}I are and the theoretical calculations are even more complex when including also this latter kind of interaction. Moreover, the simplest model scenario has been considered as well as fixed parameters values [50, 51]. Then, this case has been extended by considering some of the uncertainties which exist on the astrophysical velocity distribution [52, 22] and the physical constraint which arises from the upper limits on recoils measured by the same set-up [22]. More recently an investigation on the effect induced on the result by different possible consistent halo models still for the particular case of purely SI coupled WIMPs has also been carried out in ref. [17]. Moreover, some of the other possible scenarios have also been considered such as extensions to the general case of WIMPs with both spin-independent (SI) and spin-dependent (SD) coupling [42] [7] and to the case of WIMPs with preferred inelastic scattering [54]. In these latter cases, the effect of the uncertainties on some of the parameters has been included,

[6] We remark that a model framework is identified not only by general astrophysical, nuclear and particle physics assumptions, but also by the set of values used for all the parameters needed in the model itself and in related quantities (for example WIMP local velocity, v_0, form factor parameters, etc.).

[7] We remind that a SD component is possible also for the particular case of the neutralino since in supersymmetric theories both the squark and the Higgs bosons exchanges give contribution to the SI part of the neutralino cross section, while the squark and the Z^0 exchanges give contribution to the SD one.

but still only the simplified, approximate and non-consistent isothermal halo model has been considered in the calculations, since these analyses were performed before the detailed investigation on consistent halo models which has been applied to the case of ref. [17].

5.2.1 WIMPs with dominant SI interaction in a given model framework

As first scenario a full energy and time correlation analysis – properly accounting for the physical constraint arising from the measured upper limit on recoils [39, 53] – has been carried out in the framework of a given model for purely spin-independent coupled candidates with mass above 30 GeV [8]. A standard maximum likelihood method has been used. Note that different model frameworks (see above) vary the theoretical expectations and, therefore, the best fit values of cross section and mass (as well as the allowed region) also vary [9]. In particular, the inclusion of the uncertainties associated to the models and to every parameter in the models themselves as well as other possible scenarios largely enlarges the allowed region as discussed e.g. in ref. [52] for the particular case of the astrophysical velocities [10] and offers very large sets of best fit values.

As mentioned, more recently possible departures from the isothermal sphere model, which is the parameterisation usually adopted to describe the halo although approximate and non-consistent, have been investigated in a systematic way. Modifications arising from various matter density profiles, effects due to anisotropies of the velocity dispersion tensor and rotation of the galactic halo have been specifically investigated. In particular, halo models with potential and matter density having a spherical symmetry have been investigated as well as halo models with spherical symmetry but anisotropic

[8] This bound being inspired by the lower bound on the supersymmetric candidate, as derived from the LEP data in the usually adopted supersymmetric schemes based on GUT unification assumptions.

[9] It is worth to note that the exclusion plots (quoted by experiments exploiting approaches unable to investigate a model independent signature) are always dependent on the used model frameworks and several assumptions; thus, they have not an "universal" validity and must be considered cautiously in comparison with other results.

[10] For example, for the particular model framework and assumptions of ref. [22] by varying the WIMP local velocity, v_0, from 170 km/s to 270 km/s to account for its present uncertainty, we obtained the best fit values $m_W = (72^{+18}_{-15})$ GeV and $\xi\sigma_{SI} = (5.7 \pm 1.1) \cdot 10^{-6}$ pb for $v_0 = 170$ km/s and $m_W = (43^{+12}_{-9})$ GeV and $\xi\sigma_{SI} = (5.4 \pm 1.0) \cdot 10^{-6}$ pb for $v_0 = 220$ km/s. Here, ξ is the WIMP local density in 0.3 GeV cm^{-3} unit, σ_{SI} is the point-like SI WIMP-nucleon generalized cross section and m_W is the WIMP mass.

WIMP velocity distribution and halo models with axial symmetry (in these latter cases possible co-rotation or counter-rotation of the dark halo has also been considered). Some phenomenological restrictions have been applied on the considered halo models to account for the experimental observations on: *i)* the allowed values for the local rotational velocity; *ii)* the degree of flatness in the rotational curve; *iii)* the maximal values of the non-dark matter components in the Galaxy. As a result, limit values of the halo density for the considered halo models have also been obtained.

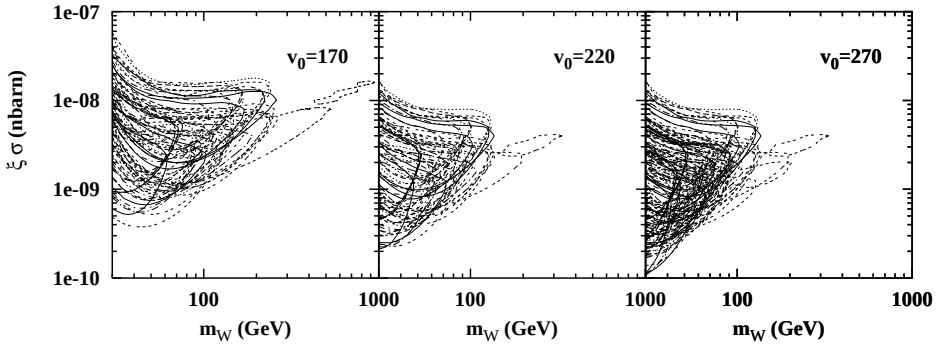

Figure 8: Superposition of the regions allowed at 3σ C.L. in the given model framework by considering the velocity distribution of each one of the halo models in ref. [17]. Three of the possible values of v_0 are considered. Obviously a specific set of best fit values for the WIMP mass and cross section corresponds to each region. Note that inclusion of other existing uncertainties will further enlarge the regions.

The global results of this analysis is shown in Fig. 8, where the allowed regions obtained for the various considered halo models in the given model framework for three of the possible values of the local velocity, v_0, are superimposed. Obviously different best fit values correspond to each one. The cumulative result, which gives a direct impact of the effect induced on the region allowed in the considered scenario only by the halo model uncertainty, is shown in Fig. 9. The obtained region is compared there with the one obtained when considering, for the given model framework, the approximate and non-consistent isothermal sphere model assuming in particular also $v_0 = 220$ km/s e $\rho_0 = 0.3$ GeV/cm^3 in the given scenario. As one can see, the cumulative 3σ C.L. allowed region is extended up to $m_W \simeq 270$ GeV with cross section on nucleon in the range $10^{-10}\text{nbarn} \leq \xi\sigma_{SI} \leq 6 \cdot 10^{-8}\text{nbarn}$.

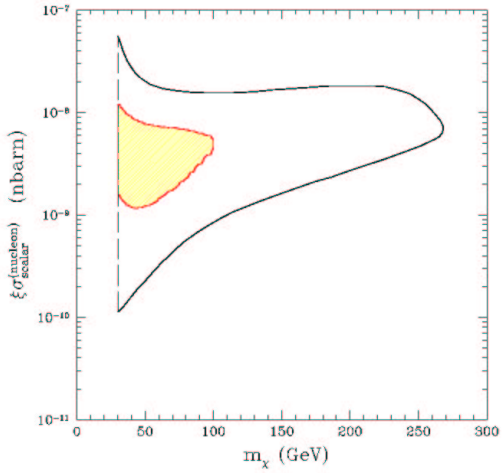

Figure 9: Region allowed at 3σ C.L. given by the superposition of all the allowed regions obtained, in the given model framework, considering several possible non-rotating halo models. Note that in these calculation only uncertainties on the halo model have been considered; the inclusion of the other existing uncertainties would further enlarge it. It is evident yhat this cumulative region, as those given e. g. in ref. [22], accounts for a large set of best fit values for WIMP mass and cross section. The shaded region, which corresponds – in the considered scenario – to the particular case of the approximate and non-consistent isothermal sphere halo model when assuming also $v_0 = 220$ km/s e $\rho_0 = 0.3$ GeV/cm^3, is shown only to point out the effect due to the poor knowledge of the right halo model. The increasing of the bound from accelerators with respect to the bound considered here will select further the possible model framework and in particular the halo models.

Maximal co-rotating and counter-rotating models can extend the allowed region up to $m_W \simeq 500 - 900$ GeV (see Fig. 8). We further stress that in this analysis no other uncertainty than the halo model [11] has been considered; the proper inclusion of the other existing uncertainties will further extend the cumulative allowed region and offer further sets of best fit values.

5.2.2 WIMPs with mixed coupling in given model framework

Since the ^{23}Na and ^{127}I nuclei are sensitive to both SI and SD couplings – on the contrary e.g. of ^{nat}Ge and ^{nat}Si which are sensitive mainly to WIMPs with SI coupling (only 7.8 % is non-zero spin isotope in ^{nat}Ge and only 4.7%

[11] Although the large number of halo models considered in this analysis, further halo models are still available and not yet considered here.

of ^{29}Si in ^{nat}Si) – the analysis of the data has been extended considering the more general case of a WIMP having not only a spin-independent, but also a spin-dependent coupling different from zero.

Then, the log-likelihood function has been minimized – properly accounting also for the physical constraint set by the measured upper limit on recoils [39] – with respect to the $\xi\sigma_{SI}$, $\xi\sigma_{SD}$ and m_W parameters for each given θ value; thus, parameters' regions allowed at given confidence level have been obtained. Here, σ_{SD} is the point-like SD WIMP cross section on nucleon and $tg\theta$ is the ratio between the effective SD coupling constants on neutrons, a_n, and on proton, a_p; therefore, θ can assume values between 0 and π depending on the SD coupling.

Note that the following results [42] have been obtained by considering there only the approximate non-consistent isothermal sphere model to describe the galactic halo and a maxwellian WIMP velocity distribution with inclusion of some uncertainties on v_0, on the nuclear radius and the nuclear surface thickness parameter in the SI form factor, on the b parameter in the used SD form factor and on the quenching factors [39] measured for the used detectors. As mentioned above, an universal formulation is not possible for the SD form factor, thus, other formulations than the one adopted here are possible and can be considered with evident implications on the obtained results.

For simplicity, Fig. 10 shows slices for some m_W of the region allowed at 3 σ C.L. in the ($\xi\sigma_{SI}$, $\xi\sigma_{SD}$, m_W) space for four particular couplings: i) θ = 0 (a_n =0 and $a_p \neq 0$ or $|a_p| >> |a_n|$); ii) $\theta = \pi/4$ ($a_p = a_n$); iii) $\theta = \pi/2$ ($a_n \neq 0$ and $a_p = 0$ or $|a_n| >> |a_p|$); iv) θ = 2.435 rad ($\frac{a_n}{a_p}$ = -0.85, pure Z^0 coupling). The case $a_p = -a_n$ is nearly similar to the case iv).

As already pointed out, when the SD contribution goes to zero (y axis in Fig. 10), an interval not compatible with zero is obtained for $\xi\sigma_{SI}$. Similarly, when the SI contribution goes to zero (x axis in Fig. 10), finite values for the SD cross section are obtained. Large regions are allowed for mixed configurations also for $\xi\sigma_{SI} \lesssim 10^{-5}$ pb and $\xi\sigma_{SD} \lesssim 1$ pb; only in the particular case of $\theta = \frac{\pi}{2}$ (that is $a_p = 0$ and $a_n \neq 0$) $\xi\sigma_{SD}$ can increase up to $\simeq$ 10 pb, since the ^{23}Na and ^{127}I nuclei have the proton as odd nucleon. Moreover, in ref. [42] we have also pointed out that: i) finite values can be allowed for $\xi\sigma_{SD}$ even when $\xi\sigma_{SI} \simeq 3 \cdot 10^{-6}$ pb as in the region allowed in the pure SI scenario considered in the previous subsection; ii) regions not compatible with zero in the $\xi\sigma_{SD}$ versus m_W plane are allowed even when $\xi\sigma_{SI}$ values much lower than those allowed in the dominant SI scenario pre-

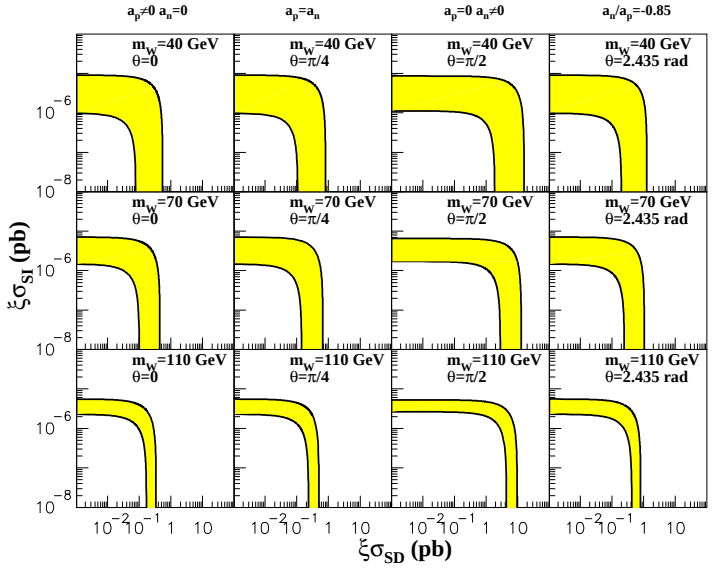

Figure 10: A mixed SI/SD case: example of slices of the region allowed at 3 σ C.L. in the ($\xi\sigma_{SI}$, $\xi\sigma_{SD}$, m_W) space for some m_W and θ values in the model framework considered in ref. [42]. Only four particular couplings are reported here for simplicity: i) $\theta = 0$; ii) $\theta = \pi/4$ iii) $\theta = \pi/2$; iv) $\theta = 2.435$ rad. Note that e.g. Ge experiments are sensitive mainly only to SI coupling and, therefore, cannot explore most of the DAMA allowed regions in this scenario. These allowed regions would be further enlarged by taking into account the uncertainties existing on the halo models and their parameters, on the SD form factor which has a not an universal formulation and on some other experimental and theoretical parameters.

viously summarized are considered; iii) best fit values with both $\xi\sigma_{SI}$ and $\xi\sigma_{SD}$ different from zero are present for some m_W and θ pairs; the related confidence level ranges between $\simeq 3\ \sigma$ and $\simeq 4\ \sigma$ [42].

Further investigations are in progress on these model dependent analyses to account for other known parameters uncertainties and for possible different model assumptions. In fact, it is worth to note that when including the uncertainties on the halo models and their parameters, on the SD form factor and on some other experimental and theoretical parameters, the allowed volume in the space ($\xi\sigma_{SI}$, $\xi\sigma_{SD}$, m_W) for each θ value would be further enlarged as well as the set of best fit values for the cross sections and the WIMP mass.

In conclusion, this analysis has shown that the DAMA data of the four annual cycles, analysed in terms of WIMP annual modulation signature, can also be compatible with a mixed scenario where both $\xi\sigma_{SI}$ and $\xi\sigma_{SD}$

are different from zero.

5.2.3 Inelastic Dark matter

It has been suggested in ref. [19] that the observed annual modulation effect could be induced by possible inelastic Dark Matter: relic particles that prefer to scatter inelastically off of nuclei. The inelastic Dark Matter could arise from a massive complex scalar split into two approximately degenerate real scalars or from a Dirac fermion split into two approximately degenerate Majorana fermions, namely χ_+ and χ_-, with a δ mass splitting. In particular, a specific model featuring a real component of the sneutrino, in which the mass splitting naturally arises, has been given in ref. [19]. It has been shown that for the χ_- inelastic scattering on target nuclei a kinematical constraint exists which favours heavy nuclei (such as ^{127}I) with respect to lighter ones (such as e.g. ^{nat}Ge) as target-detectors media. In fact, χ_- can only inelastically scatter by transitioning to χ_+ (slightly heavier state than χ_-) and this process can occur only if the χ_- velocity is larger than $v_{thr} = \sqrt{\frac{2\delta}{m_{WN}}}$ where m_{WN} is the WIMP-nucleus reduced mass ($c = 1$). This kinematical constraint becomes increasingly severe as the nucleus mass, m_N, is decreased [19]. Moreover, this model scenario gives rise – with respect to the case of WIMP elastically scattering – to an enhanced modulated component, S_m, with respect to the unmodulated one, S_0, and to largely different behaviours with energy for both S_0 and S_m (both show a higher mean value) [19].

A dedicated energy and time correlation analysis of the DAMA annual modulation data has been carried out [54] handling aspects other than the interaction type as in ref. [42] (in this way a particular model framework is fixed). As in the previous case of WIMPs with mixed SI/SD coupling, also here for simplicity a simple isothermal sphere for the galactic halo model and a maxwellian WIMP velocity distribution have been adopted, including the uncertainties on v_0. In this scenario of Dark Matter with inelastic scattering an allowed volume in the space ($\xi\sigma_p$,m_W,δ) is obtained [54]. For simplicity, Fig. 11 shows slices of such an allowed volume at some given WIMP masses (3 σ C.L.). It can be noted that when $m_W \gg m_N$, the expected differential energy spectrum is trivially dependent on m_W and in particular it is proportional to the ratio between $\xi\sigma_p$ and m_W; this particular case is summarized in the last plot of Fig. 11. The allowed regions have been obtained – as in the previous cases – by the superposition of those obtained

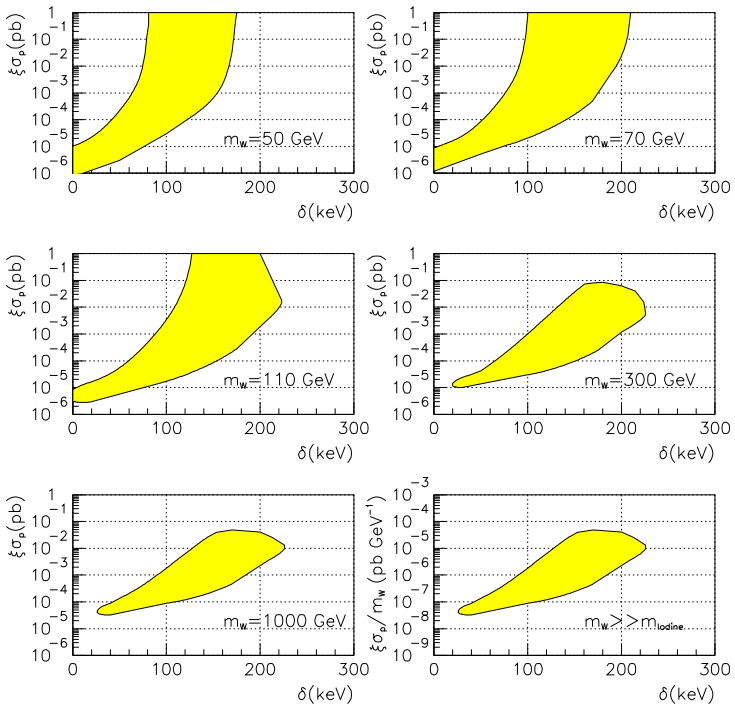

Figure 11: An inelastic case: slices at fixed WIMP masses of the volume allowed at 3 σ C.L. in the space ($\xi\sigma_p$, δ, m_W) obtained for the model framework considered in ref. [54]; some of the uncertainties on used parameters have been included [54]. Note that e.g. Ge experiments cannot explore most of the DAMA allowed regions in this scenario. These allowed regions would be further enlarged by taking into account the uncertainties existing on the halo models and their parameters and on some other experimental and theoretical parameters.

when varying the values of the previously mentioned parameters according to their uncertainties. Note that – as in the previous cases – each set of values (within those allowed by the associated uncertainties) for the previously mentioned parameters gives rise to a different expectation, thus to different "most likely" values. As an example we mention that when fixing the other parameters as in ref. [42], the "most likely" values for a WIMP mass of 70 GeV are: i) $\xi\sigma_p = 2.5 \times 10^{-2}$ pb and $\delta = 115$ keV when $v_0 = 170$ km/s, ii) $\xi\sigma_p = 6.3 \times 10^{-4}$ pb and $\delta = 122$ keV when $v_0 = 220$ km/s; they are in δ region were Ge and Si experiment are disfavoured.

Finally, we note again that the allowed regions are further enlarged when properly including the uncertainties on the halo models, on the experimental and theoretical parameters and other assumptions.

5.3 Direct detection framework

Table 1 summarizes main features for a comparison of the DAMA result with those – achieved with different methodological approaches and target nuclei – in [58, 59, 60]. Short comments can be found e.g. in [61].

6 Conclusion

There is large consensus that significant part of the Universe is in form of *cold* Dark Matter. Many experimental efforts have been carried out. The necessity of a model independent signature is evident. The efforts made by the DAMA experiment over more than one decade have pointed out the feasibility of a real experiment and the possibility of achieving physical results. This has motivated the new and increasing interest in realizing large mass set-ups for WIMP direct detection. In particular, DAMA has already collected data for other three annual cycles and the data analysis is under completion. This can allow to achieve higher confidence level for the effect and to better disentangle among different possible models. A further step in this direction will be soon realized by means of the LIBRA set-up (Large sodium Iodine Bulk for RAre processes) consisting of $\simeq$ 250 kg of highly radiopure NaI(Tl), whose installation has been now almost completed.

References

[1] F. Zwicky, *Helv. Phys. Acta* 6 (1933) 110.

[2] S. Smith, *Astrophys. J.* 83 (1936) 23.

[3] V.C. Rubin and W.K. Ford, *Astrophys. J.* 159 (1970) 379; M. Roberts and A.H. Rots, *Astron. Astrophys.* 26 (1973) 483.

[4] E.W. Kolb and M.S. Turner, "The Early Universe", Addison - Wesley (1989).

[5] J.R. Primack, *Nucl. Phys.* B (Proc. Suppl.) 87 (2000) 3 and references therein.

[6] A.H. Jaffe et al., astro-ph/0007333 (2000); J.R. Bond et al., astro-ph/0011378.

[7] A. Riess et al., *Astron. J.* 116 (1998) 1009; E.D. Perlmutter et al., *Astrophys. J.* 517 (1999) 565.

[8] R.A. Flores, *Phys. Lett.* B 215 (73) 1988 .

[9] J.M. Uson, *Nucl. Phys.* B (Proc. Suppl.) 87 (2000) 31 and references therein.

[10] P. Sikivie, *Nucl. Phys.* B (Proc. Suppl.) 87 (2000) 41.

[11] S. Cebrian et al. *Astrop. Phys.* 10 (397) 1999 ; S. Morijama et al., *Phys. Lett.* B 434 (147) 1998 .

[12] J. Preskill, *Phys. Rev. Lett.* 43 (1365) 1979 .

[13] G.D. Starkman et al., *Phys. Rev.* D 41 (3594) 1990 .

[14] R. Bernabei et al., *Phys. Rev. Lett.* 83 (4918) 1999 .

[15] F. Cappella et al., *Eur. Phys. J.*-direct C14 (2002) 1

[16] A.M. Green, *Phys. Rev.* D 63 (043005) 2001 ; N.W. Evans et al., *Mon. Not. Roy. Astron. Soc.* 318 (2000) 1131.

[17] P. Belli et al., *Phys. Rev.* D 66 (043503) 2002 .

[18] D. Fargion et al., *Pis'ma Zh. Eksp. Teor. Fiz.* 68, (*JETP Lett.* 68, 685) (1998); *Astrop. Phys.* 12 (307) 2000 .

[19] D. Smith and N. Weiner, *Phys. Rev.* D 64 (043502) 2001 .

[20] A. Bottino et al. hep-ph/9904469 (1999).

[21] A. Bottino et al., *Phys. Lett.* B 402 (113) 1997 ; *Phys. Lett.* B 423 (109) 1998 ; *Phys. Rev.* D 59 (095004) 1999 ;*Phys. Rev.* D 59 (095003) 1999 ; *Astrop. Phys.* 10 (203) 1999 ; *Astrop. Phys.* 13 (215) 2000 ; *Phys. Rev.* D 62 (056006) 2000 ; hep-ph/0010203; hep-ph/0012377.

[22] R. Bernabei et al., *Phys. Lett.* B 480 (23) 2000 .

[23] M. Ambrosio et al., *Phys. Rev.* D 60 (082002) 1999 .

[24] AMANDA Coll., *Nucl. Phys.* B (Proc. Suppl.) 87 (2000) 402; Lake Baikal Coll., *Nucl. Phys.* B (Proc. Suppl.) 87 (2000) 405; NEMO Coll., *Nucl. Phys.* B (Proc. Suppl.) 87 (2000) 433; ANTARES Coll., *Nucl. Phys.* B (Proc. Suppl.) 87 (2000) 436; NESTOR Coll., *Nucl. Phys.* B (Proc. Suppl.) 87 (2000) 448.

[25] G.L. Kane et al., *hep-ph/0108138.*

[26] R. Battiston, in the volume "Dark Matter in Astrophysics and Particle Physics" IoP (1998) 815.

[27] A. Morselli, talk given at Vulcano 2002.

[28] A. Strong et al., *Astrophys. J.* 537 (2000) 763.

[29] W. Atwood et al., *Nucl. Instr. & Methods* A 342 (302) 1994 .

[30] R. Bernabei et al., *Il Nuovo Cimento* A 112 (545) 1999 .

[31] I.R. Barabanov et al., *Nucl. Phys.* B 546 (19) 1999 .

[32] G. Heusser, *Annual Rev. of Nucl. and Part. Scie.* 45 (1995) 543.

[33] F.T. Avignone et al., *Nucl. Instr. & Methods* A 292 (37) 1990 .

[34] R. Bernabei et al., *Phys. Lett.* B 436 (1998) 379 .

[35] R. Bernabei et al., *Eur. Phys. J. direct* C11 (2001) 1.

[36] K. Fushimi et al., *Nucl. Phys.* B35 (Proc. Suppl.) (1994) 400.

[37] P. Belli et al., *Phys. Lett.* B 387 (1996) 222 ; *Phys. Lett.* B 389 (1996) 783 (err.).

[38] R. Bernabei et al., *New Journal of Physics* 2 (1) 2000 5.1.

[39] R. Bernabei et al., *Phys. Lett.* B 389 (757) 1996 .

[40] R.H. Helm, *Phys. Rev.* 104 (1466) 1956 ; A. Bottino et al., *Astrop. Phys.* 2 (77) 1994 .

[41] M.T. Ressell et al., *Phys. Rev.* C 56 (535) 1997 .

[42] R. Bernabei et al., *Phys. Lett.* B 509 (197) 2001 .

[43] C. Bacci et al., *Astrop. Phys.* 2 (117) 1994 .

[44] D.P. Snowden-Ifft et al., in the volume *The identification of Dark Matter*, World Sc. (2000) 463.

[45] P. Belli et al., *Il Nuovo Cimento* C 15 (475) 1992 .

[46] R. Bernabei et al., ROM2F/2002/34

[47] J.I. Collar and F.T. Avignone, *Phys. Lett.* B 275 (181) 1992 ; *Phys. Rev.* D 47 (5238) 1993 .

[48] R. Bernabei et al., *Il Nuovo Cimento* A 112 (1541) 1999 .

[49] K.A. Drukier et al., *Phys. Rev.* D 33 (3495) 1986 ; K. Freese et al., *Phys. Rev.* D 37 (3388) 1988 .

[50] R. Bernabei et al., *Phys. Lett.* B 424 (195) 1998 .

[51] R. Bernabei et al., *Phys. Rev.* D 450 (448) 1999 .

[52] P. Belli et al., *Phys. Rev.* D 6 (023512) 2000 .

[53] R. Bernabei et al., *Eur. Phys. J.* C18 (2000) 283.

[54] R. Bernabei el al., ROM2F/2001/33, to appear on *Eur. Phys. J.* C.

[55] R. Bernabei, *Prog. Part. Nucl. Phys.* 48 (2002) 263.

[56] P. Belli et al., *Astrop. Phys.* 5 (1996) 217 ; P. Belli et al., *Il Nuovo Cimento* C 19 (1996) 537 ; P. Belli et al., *Phys. Lett.* B 387 (1996) 222 and *Phys. Lett.* B 389 (1996) 783 (err.); R. Bernabei et al., *Astrop. Phys.* 7 (73) 1997 ; R. Bernabei et al., *Il Nuovo Cimento* A 110 (189) 1997 ; R. Bernabei et al., *Phys. Lett.* B 408 (439) 1997 ; R. Bernabei et al., *Phys. Lett.* B 436 (1998) 379 ; P. Belli et al., *Astrop. Phys.* 10 (115) 1999 ; P. Belli et al., *Phys. Lett.* B 460 (236) 1999 ; P. Belli et al., *Nucl. Phys.* B 563 (97) 1999 ; R. Bernabei et al., *Phys. Rev. Lett.* 83 (4918) 1999 ; P. Belli et al., *Phys. Rev.* C 60 (065501) 1999 ; P. Belli et al., *Phys. Lett.* B 465 (1999) 315 ; P. Belli et al., *Phys. Rev.* D 61 (2000) 117301 ; R. Bernabei et al., *New Journal of Physics* 2 (2000) 15.1 ; R. Bernabei et al., *Phys. Lett.* B 493 (2000) 12 ; R. Bernabei et al., *Phys. Lett.* B 515 (6) 2001 ; R. Bernabei et al., *Eur. Phys. J. direct* C11 (2001) 1; R. Bernabei et al., *Phys. Lett.* B 527 (182) 2002 ; R. Bernabei et al., *Nucl. Phys.* A 705 (2002) 29 ; R. Bernabei, *Prog. Part. Nucl. Phys.* 48 (2002) 263; R. Bernabei et al., INFN/AE-01/19, to appear on XENON-01, World Sci. Pub.; R. Bernabei et al., *Phys. Lett.* B 546 (23) 2002 .

[57] R. Bernabei et al., *Nucl. Instr. & Methods* A 482 (728) 2002 .

[58] CDMS collaboration, *Phys. Rev. Lett.* 84 (5699) 2000 .

[59] EDELWEISS collaboration, *Phys. Lett.* B 513 (15) 2001 .

[60] N. Smith, talk given at IDM02, York, september 2002

[61] P. Belli et al., in the volume "Relativistic Astrophysics", 20th Texas Symp., AIP (2001) 95; astrop-ph/0205047 to appear in the Proc. of "Dark2002" Cape Town, South Africa, 2002; ROM2F/2002/26 to appear in the Proc. of "Beyond the Desert 2002", Oulu, Finland, available on DAMA homepage on http://www.lngs.infn.it.

Table 1: Comparison of some features of DAMA/NaI, CDMS-I, Edelweiss-I, UKLXe (Zeplin-I)

	DAMA/NaI	CDMS-I	Edelweiss-I	UKLXe (Zeplin-I)
Signature	annual modulation	None	None	None
Target-nuclei	^{23}Na, ^{127}I	^{nat}Ge	^{nat}Ge	^{nat}Xe
Technique	well known	poorly experienced	poorly experienced	optical interface liquid/gas in this realization
Target mass	$\simeq$ 100 kg	0.5 kg	0.32 kg	$\simeq$ 3 kg
Exposure	57986 kg $\times$ day (+3 other cycles at hand)	15.8 kg $\times$ day	8.2 kg $\times$ day	230 kg $\times$ day
Depth of the experimental site	1400 m	10 m	1700 m	1100 m
Software energy threshold	2 keVee	10 keVee	20 keVee	2 keVee (but: $\sigma/E = 100\%$ and 1 p.e./keV)
Quenching factor	Measured	Assumed = 1	Assumed = 1	Measured
Measured event rate in low energy range	$\simeq$ 1 cpd/kg/keV	$\simeq$ 60 cpd/kg/keV (10^5 events)	2500 events total	$\simeq$ 100 cpd/kg/keV
Claimed events after rejection procedures		23 in Ge, 4 in Si, 4 multiple events in Ge + MonteCarlo on neutron flux	0	$\simeq$ 40 cpd/kg/keV after rejection and ?? after PSD
Events satisfying the signature in DAMA/NaI	modulation amplitude integrated over the given exposure $\simeq$ 2000 events			
Expected number of events from DAMA/NaI effect		from few down to zero depending on the models (and on quenching factor)	from few down to zero depending on the models (and on quenching factor)	depends on the models (even zero)